Scientific Reports

https://doi.org/10.1038/s41598-026-37139-0

Article in Press

Biogenic synthesis of iron nanoparticles using *Laurencia papillosa*: characterization, optimization, and dual applications in heavy metal removal and potential cancer treatment

Received: 1 October 2025

Accepted: 20 January 2026

Published online: 18 February 2026

Cite this article as: El Shehawy A.S., Elsayed A. & Ali E.M. Biogenic synthesis of iron nanoparticles using *Laurencia papillosa*: characterization, optimization, and dual applications in heavy metal removal and potential cancer treatment. *Sci Rep* (2026). https://doi.org/10.1038/s41598-026-37139-0

Ahlam S. El Shehawy, Ashraf Elsayed & Elham M. Ali

We are providing an unedited version of this manuscript to give early access to its findings. Before final publication, the manuscript will undergo further editing. Please note there may be errors present which affect the content, and all legal disclaimers apply.

If this paper is publishing under a Transparent Peer Review model then Peer Review reports will publish with the final article.

ARTICLE IN PRESS

© The Author(s) 2026. **Open Access** This article is licensed under a Creative Commons Attribution 4.0 International License, which permits use, sharing, adaptation, distribution and reproduction in any medium or format, as long as you give appropriate credit to the original author(s) and the source, provide a link to the Creative Commons licence, and indicate if changes were made. The images or other third party material in this article are included in the article's Creative Commons licence, unless indicated otherwise in a credit line to the material. If material is not included in the article's Creative Commons licence and your intended use is not permitted by statutory regulation or exceeds the permitted use, you will need to obtain permission directly from the copyright holder. To view a copy of this licence, visit http://creativecommons.org/licenses/by/4.0/.

ARTICLE IN PRESS

Biogenic Synthesis of Iron Nanoparticles Using *Laurencia papillosa*: Characterization, Optimization, and Dual Applications in Heavy Metal Removal and Potential Cancer Treatment

Ahlam S. El Shehawy[a,*], Ashraf Elsayed [a,*], Elham M. Ali[b,c]

[a] Department of Botany, Faculty of Sciences, University of Mansoura, Egypt.

[b] Department of Aquatic Environment, Faculty of Fish Resources, University of Suez, Egypt.

[c] Department of Environmental Studies, The National Authority for Remote Sensing and Space Sciences (NARSS), Egypt.

***Corresponding Author:** ahlam.saleh@outlook.com
ashraf-badawy@mans.edu.eg

Abstract

The present study explores the biogenic synthesis of iron nanoparticles (FeNPs) using the red marine alga *Laurencia papillosa*, aiming to evaluate their dual potential in environmental remediation and cancer treatment. The FeNPs were synthesized under optimized conditions determined by response surface methodology (RSM), pH 7.0, 20 g/100 mL algal concentration, and 24 hours, ensuring maximum yield and reproducibility. The synthesized FeNPs were characterized using X-ray Diffraction (XRD), FTIR, TEM, SAED, SEM, EDAX, and zeta potential analysis, revealing spherical, polydispersed particles with sizes ranging from 10.17 to 19.99 nm and a zeta potential of +7.4 mV, indicating moderate stability. Optimization of synthesis conditions using a response surface methodology (RSM) model identified pH 7.0, 20 g/100 mL algal concentration, and 24 hours as optimal for maximum nanoparticle yield. The FeNPs demonstrated remarkable efficacy in removing heavy metals from aquaculture wastewater, with removal efficiencies of 96.4% for Fe, 58.3% for Mn, and 23.1% for Zn. Additionally, in vitro cytotoxicity assays demonstrated dose-dependent inhibitory effects against Human liver (HepG2) and Breast (MDA-MB-231) cancer cell lines, confirming the potential biomedical application of these eco-friendly FeNPs. These

ARTICLE IN PRESS

findings highlight the unique capability of *L. papillosa*-mediated FeNPs as multifunctional nanomaterials, bridging sustainable environmental remediation with cancer therapeutics, offering promising prospects for sustainable nanotechnology in both environmental and biomedical fields. Overall, the study demonstrates that *L. papillosa* derived FeNPs combine optimized green synthesis, effective heavy metal removal, and notable anticancer activity, underscoring their potential as cost-effective and environmentally sustainable multifunctional nanomaterials.

Keywords: Iron nanoparticles, *Laurencia papillosa*, Green synthesis, Nanoparticles, Heavy metal removal, Cytotoxicity.

1. Introduction

Nanotechnology is one of the top technologies that offers great potential for many problems, among them, the development of next-generation wastewater treatment approaches [1,2] and biomedicine [3,4]. Among the various nanoparticles developed, iron nanoparticles (FeNPs) have attracted significant attention due to their high magnetic nature, high surface area, redox potential, low toxicity, and simple separation methodology [5,6]. These features make them highly versatile for addressing pressing global challenges like water pollution and cancer treatment.

However, conventional methods for synthesizing FeNPs often require high cost and energy and involve toxic chemicals and organic solvents, which can be hazardous to humans and the environment, raising concerns about their environmental sustainability and biocompatibility [7]. In response to these challenges, biogenic synthesis has gained momentum as a green and sustainable alternative [8]. Algae, particularly marine seaweed, have shown promise due to their abundant secondary metabolites, such as polysaccharides, phenolics, proteins, terpenoids, and flavonoids, which can act as natural reducing, capping, and stabilizing agents during nanoparticle formation [1]. These bioactive compounds not only facilitate rapid nucleation and growth of nanoparticles but also enhance their stability and prevent aggregation [9]. Seaweed-mediated green synthesis offers several advantages, including stability, low-temperature synthesis,

ARTICLE IN PRESS

energy efficiency, reduced toxicity, and environmental safety [10]. Additionally, this approach is cost-effective, scalable, and capable of producing nanoparticles with controlled size, morphology, and surface properties, making it highly suitable for applications in environmental remediation, biomedicine, and industrial nanotechnology [11], as highlighted in Figure 1. Previous studies have demonstrated the successful use of seaweeds, particularly red algae, in the biogenic synthesis of metallic nanoparticles due to their rich content of sulfated polysaccharides and phenolic compounds [2]. Red algae of the genus *Laurencia* have received increasing attention, as they are known to produce diverse bioactive metabolites that facilitate efficient nanoparticle formation with controlled size and morphology. Several studies have reported the synthesis of silver [3], gold [4], and iron-based nanoparticles [5] using *Laurencia* spp., showing enhanced stability, antimicrobial activity, and catalytic performance. These findings established red seaweeds as reliable and eco-friendly nanofactories, paving the way for their exploration in multifunctional applications beyond conventional antimicrobial uses**.**

The red alga *Laurencia papillosa* is a potent candidate for biogenic nanoparticle synthesis due to its rich biochemical composition and ecological abundance [12]. *L. papillosa* exhibits unique biochemical traits that distinguish it from other algae commonly utilized in FeNPs biosynthesis. It is particularly enriched with halogenated secondary metabolites, sulfated polysaccharides, terpenoids, and phenolic compounds, which together provide strong reducing capacity and enhanced capping activity during nanoparticle formation [6]. Compared with genera such as *Ulva*, *Sargassum*, and *Chlorella*, the distinctive halogenated compounds and high antioxidant potential of *L. papillosa* may contribute to superior nanoparticle stability, uniformity, and bioactivity [7,8].

ARTICLE IN PRESS

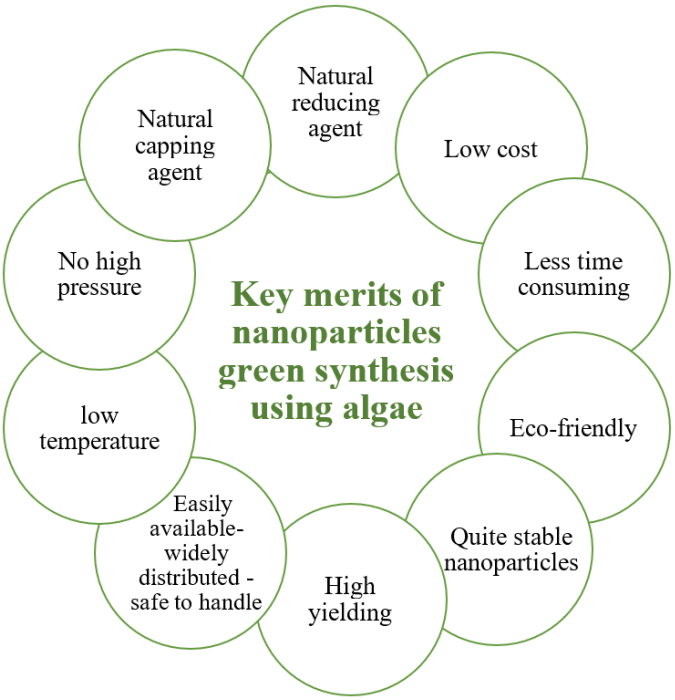


Fig. 1. Key merits of NPs green synthesis using algae.

Water-related problems are a persistent global issue and most hydrological resources have been under pressure due to several factors, including population growth, urbanization, and industrialization [13]. More than 14,000 people per day globally die from diseases and conditions caused by water pollution [14]. Heavy metals contribute significantly to water pollution, disrupting ecological balance and posing serious environmental and health risks, which calls for developing efficient and cost-effective remediation strategies [15]. On the other hand, cancer causes about 1 in every 6 deaths worldwide, and it is the second-leading cause of death worldwide [16]. Nanoparticles have been reported as promising anticancer agents, offering an alternative to traditional methods that often rely on targeted drug delivery and controlled-release technologies, which can be more harmful [17]. Their effectiveness has been demonstrated against various cancer cell lines, including human liver carcinoma cells (HepG2) [18], breast cancer cell line (MCF-7) [19][9], colon cancer [20], and cervical cancer [21].

Although numerous studies have reported the synthesis of iron nanoparticles (FeNPs) using chemical or biological methods, most rely on terrestrial plants or microorganisms and primarily focus on single-purpose

ARTICLE IN PRESS

applications. In contrast, the use of the marine red alga *Laurencia papillosa* for FeNP synthesis remains largely unexplored, despite its rich content of bioactive metabolites that can act as effective reducing and stabilizing agents. Therefore, this study addresses a clear knowledge gap by developing an eco-friendly and cost-effective biogenic synthesis of FeNPs using *Laurencia papillosa*, followed by systematic characterization and optimization of synthesis parameters. Furthermore, unlike previous studies that examine either environmental or biomedical applications separately, the synthesized FeNPs are evaluated for their dual functionality in heavy metal removal and anticancer activity, highlighting their multifunctional potential.

2. Materials and methods

2.1. Biogenic Synthesis of FeNPs

The marine seaweed *Laurencia papillosa* was hand-collected from Zaafarana Beach (29.06° N, 32.43° E), Suez Gulf, Red Sea, Egypt. The algae were identified by keeping some of the fresh seaweeds in seawater containing 5% formalin and classified according to [22]. The samples were air-dried in a shaded area for two weeks. The aqueous algal extract was prepared by soaking 5 g of dry algal powder in 100 mL of deionized water for 24 hours with frequent shaking, followed by filtration through Whatman Filter paper No. 1. The supernatant was then used to prepare FeNPs [10]. All chemicals and reagents used in this study were of analytical grade and used without further purification. Ferric chloride ($FeCl_3$, ≥99% purity) was obtained from Sigma, Egypt. Deionized water was used throughout all experiments. FeNPs were synthesized by mixing algal extract with a 0.1 M $FeCl_3$ solution in a 1:1 volume ratio. The mixture was stirred for one hour and maintained at room temperature (~25 °C), and then left at the same temperature for 30 minutes to allow complete nanoparticle formation [8]. The resulting FeNPs were collected by centrifugation at 10,000 rpm for 15 min, washed with absolute ethanol to remove unreacted biomolecules and impurities, and then rinsed three

ARTICLE IN PRESS

times with deionized water to ensure purity. The purified FeNPs were finally dried and stored for further characterization and analysis [23].

2.2. Characterization of Biogenic FeNPs

The crystal structure, phase composition, and crystallite size of FeNPs were detected using X-ray Diffraction (XRD). It was obtained by a DX-1000 X-ray powder diffractometer operated at 40 kV and 30 mA, in the 2θ range of 10°-90° [11]. Fourier Transform Infrared (FTIR) spectroscopy was employed to identify biomolecules involved in nanoparticle synthesis by analyzing functional groups in the range of 400-4000 cm^{-1} using Burker Vertex 80 (Germany) to determine the main components of algal extracts and determine the biomolecules involved in the synthesis of FeNPs [24]. Transmission Electron Microscopy (TEM) was used to examine nanoparticle size, shape, and internal structure, while Selected Area Electron Diffraction [12] [12] analysis provided information on crystallinity and lattice characteristics that can be performed inside a transmission electron microscope [25]. Scanning Electron Microscopy (SEM) was utilized to investigate surface morphology and particle distribution by using the powder form of FeNPs, which was cast onto glass slides, followed by fixation on copper supports. The samples were covered with a thin layer of gold by sputtering. The coated surface was examined using SEM (JEOL JSM-6510LV, Japan, high resolution of 3.0 nm at 30 kV) [13]. The elemental composition of the FeNPs was analyzed using Energy Dispersive X-ray Analysis (EDAX) coupled with SEM [26]. Colloidal stability and surface charge of the nanoparticles were assessed through zeta potential measurements using Photon Correlation Spectroscopy [27].

2.3. Optimization of Biogenic FeNPs Synthesis using Central Composite Design (CCD)

Response Surface Methodology (RSM) was utilized to evaluate the effects of key factors: pH, algal extract concentration (g/100 mL), and reaction time (h) on the biogenic synthesis of FeNPs from *L. papillosa*. CCD was utilized to determine the optimum level of each variable for FeNPs synthesis, through defining the main effects and interaction between the different selected three factors at five levels, including five replicates at

ARTICLE IN PRESS

the center point. This was applied to fit the data into a second-order quadratic polynomial model [28].

A total of 20 runs were conducted, each in triplicate, with absorbance at 300 nm measured via UV-Vis spectrophotometry to monitor Surface Plasmon Resonance (SPR), which served as an indirect indicator of FeNPs formation and concentration**.** Analysis of variance (ANOVA) was evaluated by statistical analysis of the model by the Design Expert 8.0 statistical package (StatEase, Inc., Minneapolis, MN, USA). To demonstrate the interaction between variables, the surface plots of 3-D surface designs were plotted that describe each parameter's optimal condition for the development of biogenic FeNPs. Normal probability plots of residuals and residuals versus predicted values were analyzed for each response variable to assess model adequacy, determine optimal conditions, and validate the experimental design using Design-Expert software.

Table 1. Levels of variables used in the Central Composite Design (CCD) experiment for the synthesis of biogenic FeNPs.

Variables	**Levels**				
	-2	-1	0	+1	+2
pH	3.0	4.9	7.0	9.4	11.0
The concentration of algae extract (g/100 ml)	1.0	4.9	10.5	16.1	20
Time (h)	1	10.5	24	38.5	48

ARTICLE IN PRESS

2.4. Heavy Metal (Fe, Mn, and Zn) Removal from Fish Aquaculture Wastewater Effluents using Biogenic FeNPs

Wastewater samples were collected from the effluents of a running aquaculture facility in Port Said Governorate, Egypt (31°19'41"N, 32°25'22"E). For the removal experiment, 100 mL of filtered wastewater was mixed with 0.2 g/L FeNPs and stirred at 120 rpm at 25°C for 90 minutes. The FeNPs were then separated by centrifugation at 4000 rpm for 15 minutes. Heavy metal concentrations were measured before and after treatment using an atomic absorption spectrophotometer. The removal efficiency (%R) for each metal was calculated using the equation [29]:

ARTICLE IN PRESS

$$\%R = \frac{C_0 - C_t}{C_0} \times 100$$

where C_o is the initial metal concentration (mg/L), and C_t is the concentration after treatment (mg/L).

2.5. Evaluation of Antitumor Activity of Biogenic FeNPs

The central lab in the zoology department, Faculty of Science, Mansoura University, Egypt, provided cell lines of Human liver (HepG2) cells and Human Breast Cancer Cell Line (MDA-MB-231). The cytotoxicity of FeNPs was evaluated by 3-(4,5-dimethylthiazol-2-yl)- 2,5-diphenyltetrazolium bromide (MTT) dye reduction assay [30]. In brief, HepG2 cells and MDA-MB-231 were harvested, seeded in a 96-well plate, and exposed to different concentrations (0.5, 1, 2, 4, 8, and 16 µg/mL) of FeNPs for 24 h at 37°C in 5% CO_2. After the treatment, the medium was aspirated, and the treated cells were exposed to 10 µl of MTT for another 2h in the dark at 37°C. At the end of the incubation period, the purple formazan crystals were solubilized with 50 µl DMSO and measured spectrophotometrically on a microplate reader at 595 nm. The percentage of viable cells was calculated as follows [31]:

$$\text{Cell viability percentage} = \left(\frac{\text{OD of treated cells}}{\text{OD of untreated cells}}\right) \times 100$$

The IC_{50} of HepG2 and MDA-MB-231 doses was calculated by Prism software.

3. Results

Before the biogenic synthesis of FeNPs, the algal samples collected from Zaafarana Beach, located along the Red Sea coast in Egypt (Fig. 2a), were carefully examined and taxonomically classified [22]. *Laurencia papillosa* was confirmed as a red alga belonging to the Rhodophyta phylum (Fig. 2b). algal biomass was subjected to shadow drying to preserve its bioactive compounds (Fig. 2c) and then finely ground to facilitate subsequent extraction and nanoparticle synthesis processes (Fig. 2d).

ARTICLE IN PRESS

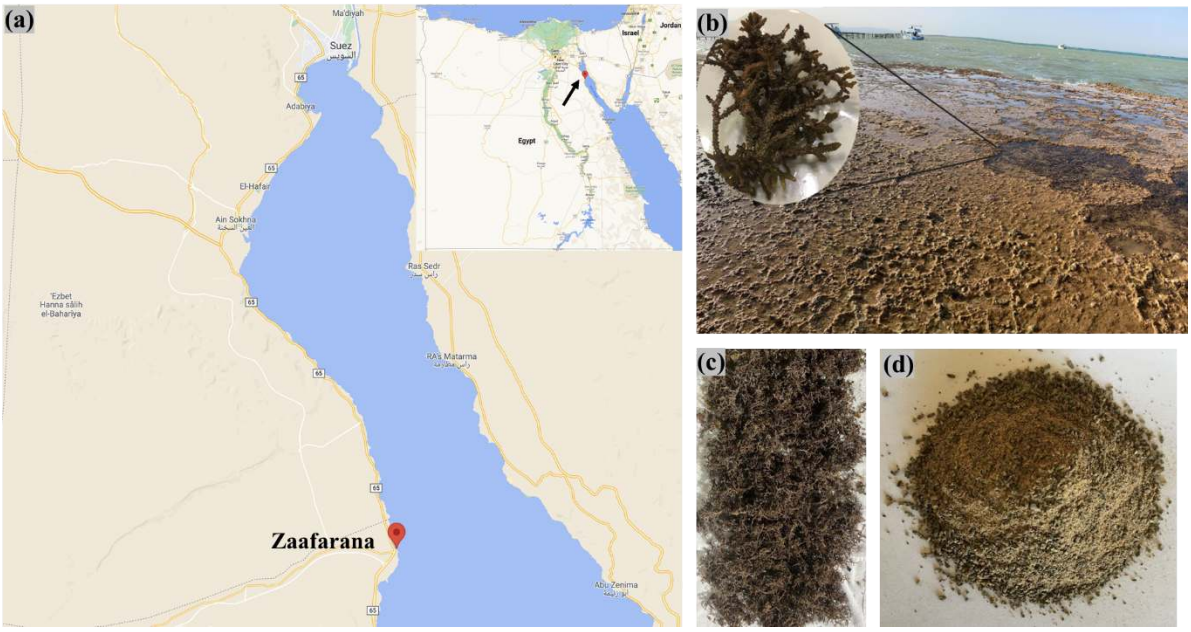


Fig. 2. (a) Location map of the algal collection site at Zaafarana Beach, Red Sea, Egypt; **(b)** Photographs of the site and the harvested *Laurencia papillosa*; **(c)** Algal samples during shadow drying; and **(d)** Ground algal material.

3.1. X-ray Diffraction and Fourier Transform Infrared Spectroscopy Analysis

The XRD pattern of biogenic FeNPs gives amorphous nanoparticles (Fig. 3a). The inset image provides initial evidence of FeNP formation, as indicated by the color change of the algal extract from yellowish-brown to deep brown upon the addition of $FeCl_3$ solution. FTIR spectra of both biogenic FeNPs and *L. papillosa* extract (Fig. 3b) were recorded within the 4000-400 cm^{-1} range. Prominent peaks were observed at 3421, 1598, 1384, 1035, and 865 cm^{-1}. While the overall spectral pattern of *L. papillosa* extract and FeNPs remained similar, variations in peak intensity were noted.

ARTICLE IN PRESS

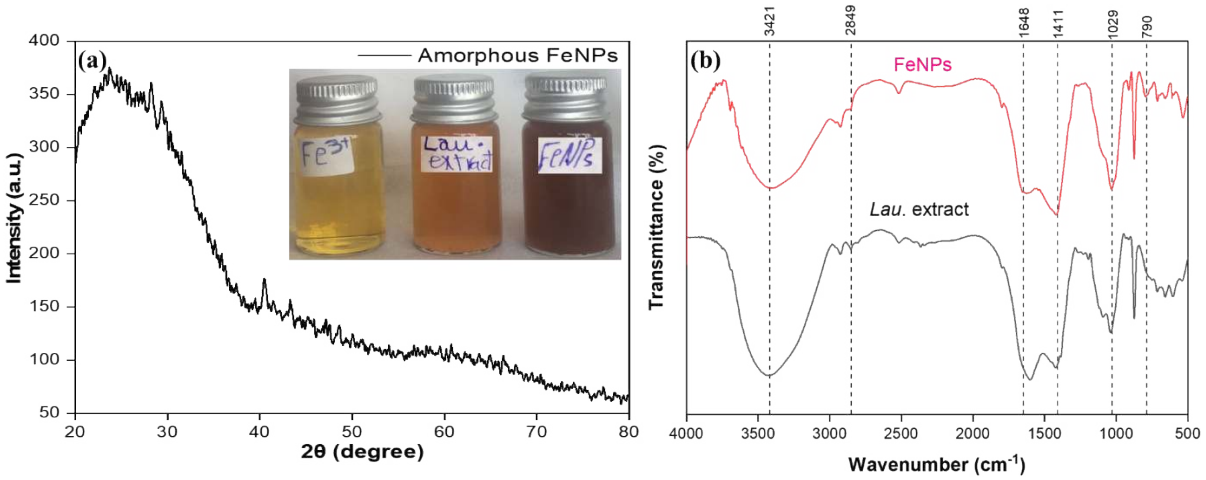


Fig. 3. (a) XRD patterns of biogenic FeNPs; inset: algal extract before and after exposure to $FeCl_3$ solution. **(b)** FTIR spectra of FeNPs and *Laurencia papillosa* extract.

3.2. Structural Characterization of Biogenic FeNPs

The TEM micrographs presented in Fig. 4a and b, FeNPs are nearly spherical with approximately poly-dispersed particles. The particle size of FeNPs was observed to range from 10.17 to 19.99 nm. The inset micrographs in Fig. 4c showed that the SAED patterns exhibit alternating dots and concentric rings, demonstrating that FeNPs are polycrystalline.

Figure 4d shows the EDAX spectra of FeNPs, where the peaks at 0.5, 6.0, and 6.6 keV are related to the binding energies of Fe. In addition to the Fe peak, the EDAX spectrum shows minor peaks corresponding to C, O, Na, Mg, Al, Cl, K, Cu, and Zn. These elements likely originate from residual biomolecules and trace salts present in the *Laurencia papillosa* extract. The SEM analysis was conducted to know the surface morphology of FeNPs, where the particle shapes were spherical, highly distributed, and polydispersed (Fig. 4e and f). The FeNPs exhibited a positive zeta potential of +7.4 mV (Fig. 4g), indicating the presence of a positively charged nanoparticle surface and moderate dispersion stability under the experimental conditions.

ARTICLE IN PRESS

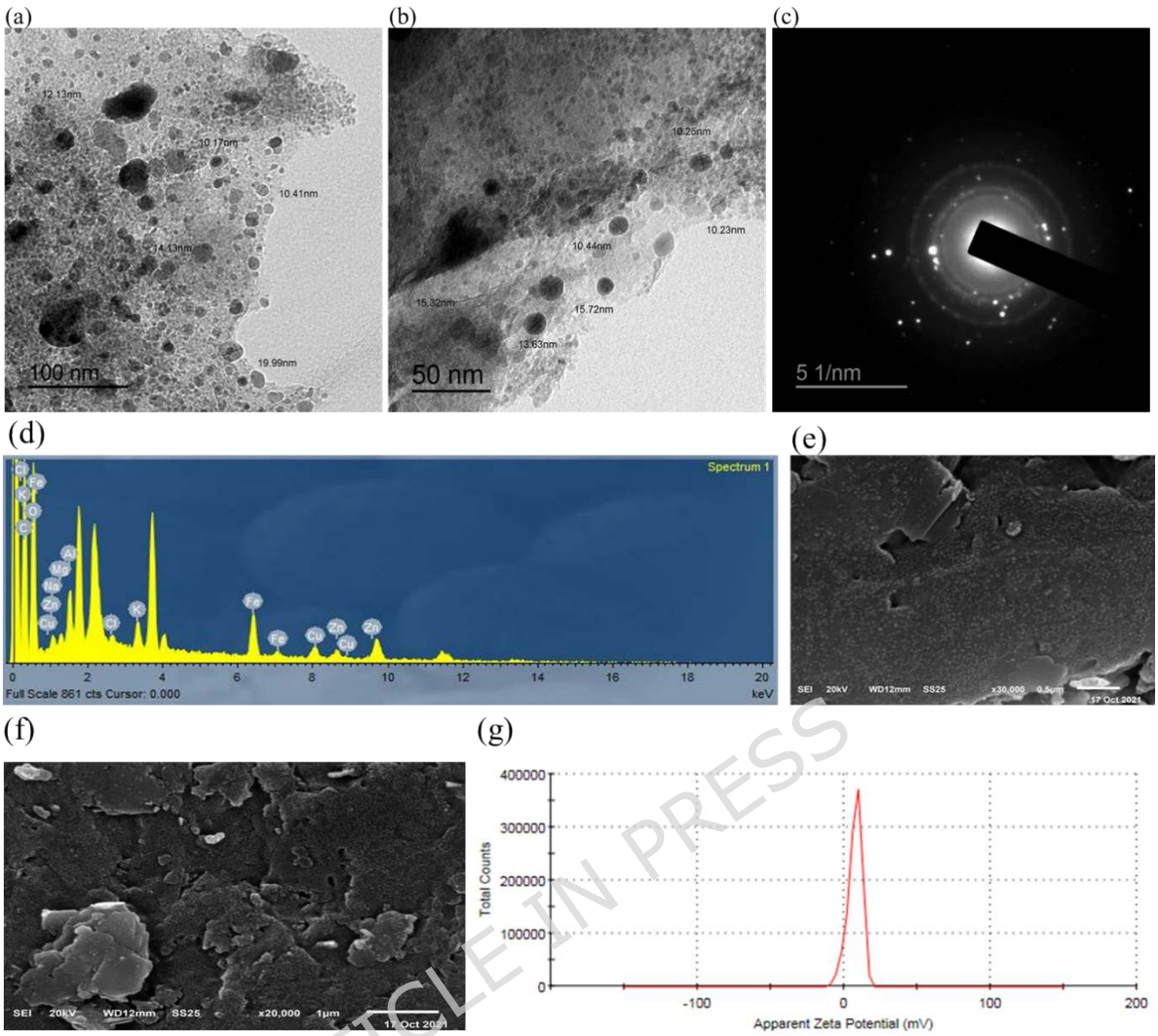


Fig. 4. (a) TEM image at 100 nm, (b) TEM image at 50 nm, (c) SAED pattern, (d) EDX spectrum analysis, (e) SEM image at 30,000× magnification, (f) SEM image at 20,000× magnification, and (g) zeta potential of biogenic FeNPs.

3.3. Optimizing conditions for biogenic synthesis of FeNPs

Twenty experiments optimized the phyco-synthesis of FeNPs from *Laurencia papillosa*, quantified by SPR intensity (Table 2). The optimal conditions (Run No. 16) were pH 7.0, 20 g algae/100 mL water, and 24 hours, yielding a maximum absorbance of 1.30 at 300 nm. ANOVA confirmed a significant quadratic model ($P < 0.05$), with pH and concentration as key factors, while time was non-significant (Table 3).

ARTICLE IN PRESS

Table 2. Specifics of the 20 runs that were carried out utilizing CDD to improve the biogenic synthesis of FeNPs using *Laurencia papillosa* extract.

Runs	Variables			Responses
	pH	The concentration of algal extract (g/100 mL)	Incubation time (h)	SPR_{300}
1	4.6	4.9	10	0.64
2	9.4	4.9	10	1.08
3	4.6	16.1	10	0.76
4	9.4	16.1	10	0.78
5	4.6	4.9	38	0.58
6	9.4	4.9	38	0.64
7	4.6	16.1	38	0.85
8	9.4	16.1	38	1.14
9	7	10.5	24	1.04
10	7	10.5	24	0.54
11	7	10.5	24	0.80
12	7	10.5	24	0.91
13	3	10.5	24	0.77
14	11	10.5	24	0.69
15	7	1.0	24	0.84
16	**7**	**20.0**	**24**	**1.30**
17	7	10.5	1	0.78
18	7	10.5	48	0.90
19	7	10.5	24	0.95
20	7	10.5	24	0.7

ARTICLE IN PRESS

Table 3. The full quadratic model's ANOVA and model performance of biogenic synthesis of FeNPs using *Laurencia papillosa* extract.

Source	Sum of Squares	df	Mean Square	F-value	p-value	
Model	0.6081	9	0.0676	4.51	0.0138	significant
A-pH	0.0807	1	0.0807	5.39	0.0427	
B-Conc	0.1565	1	0.1565	10.44	0.0090	
C-Time	0.0005	1	0.0005	0.0321	0.8614	
AB	0.0023	1	0.0023	0.1543	0.7027	
AC	0.0039	1	0.0039	0.2584	0.6223	

ARTICLE IN PRESS

BC	0.1280	1	0.1280	8.54	0.0152	
A^2	0.1627	1	0.1627	10.86	0.0081	
B^2	0.0594	1	0.0594	3.96	0.0745	
C^2	0.0043	1	0.0043	0.2859	0.6045	
Residual	0.1499	10	0.0150			
Lack of Fit	0.0890	5	0.0178	1.46	0.3437	not significant
Pure Error	0.0609	5	0.0122			
Cor Total	0.7580	19				

Figure 5 shows the 3D response surface plots that represent the effect of pH, Conc, and time on the SPR intensity of FeNPs. Figures 5a and b show that concentration and pH have a higher impact on SPR intensity than time. In addition, concentration had the greatest impact on the synthesis of AgNPs (Figure 5c). The assumption of normal data is shown in Figure 5d. The data were almost normal, and the graph showed the normal probability of how the residues followed a normal distribution. Figure 5e presents the relation of residual vs. predicted SPR intensity. It shows that the residual is randomly distributed on both sides of the zero line and also lies in a range less than the allowable range of $\pm 3\sigma$.

ARTICLE IN PRESS

ARTICLE IN PRESS

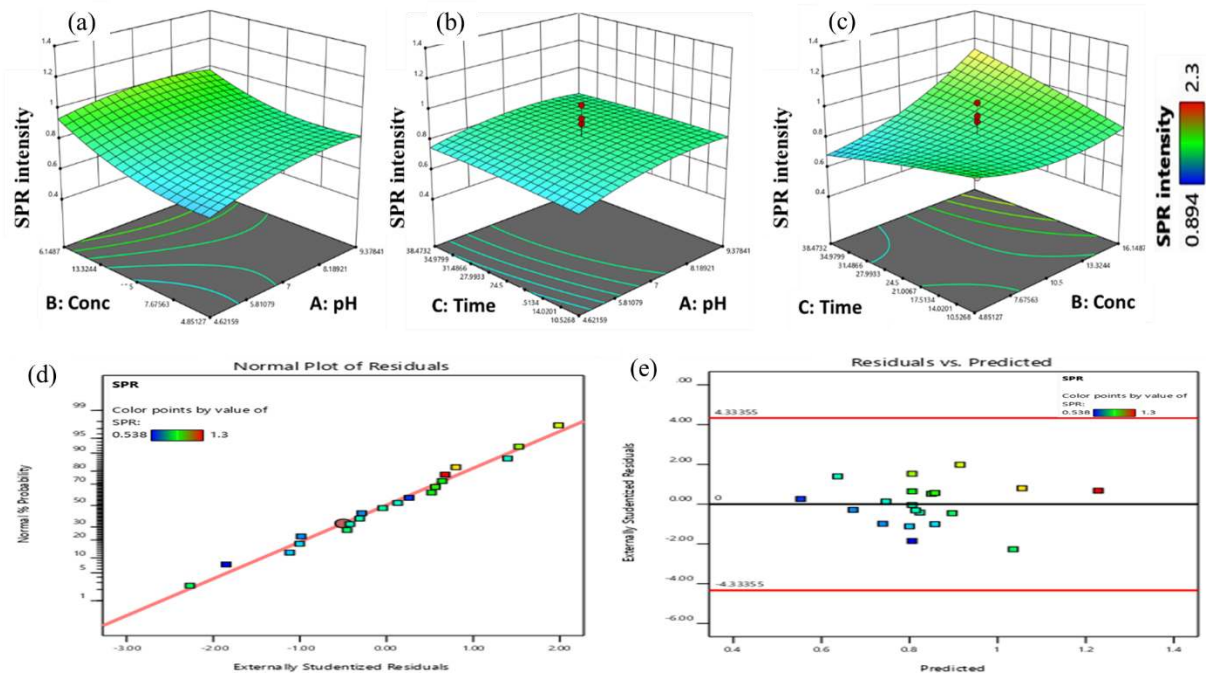


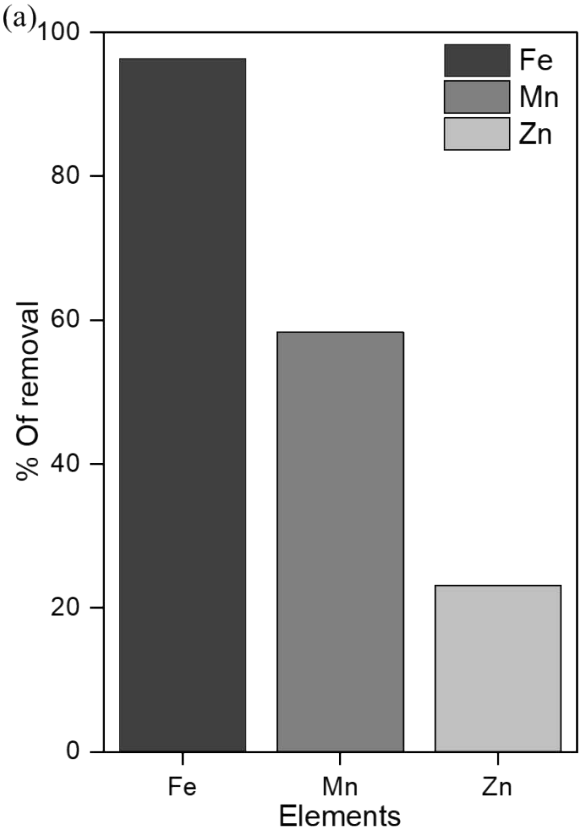
Fig. 5. (a) Three-dimensional response surface plots illustrating the effects of independent parameters: [concentration–pH], (b) [pH–time], and (c) [time–concentration] on SPR intensity under optimal conditions for the biogenic synthesis of FeNPs using *Laurencia papillosa* extract. (d) Normal probability plot of internally studentized residuals for the quadratic model of SPR intensity. (e) Residuals versus predicted SPR intensity for the biogenic synthesis of FeNPs using *Laurencia papillosa* extract.

3.4. Effectiveness of FeNPs in Heavy Metal Removal

As illustrated in Figure 6a, treating aquaculture wastewater effluent with biogenic FeNPs significantly reduced iron concentrations, achieving a removal efficiency of 96.4%. The treatment also decreased manganese and zinc levels, with removal efficiencies of 58.3% and 23.1%, respectively. In support of these findings, the concentration table (Figure 6b) displays the exact values of Fe, Mn, and Zn before and after treatment, confirming a substantial decline in heavy metal concentrations post-treatment.

ARTICLE IN PRESS

(a)



(b)

Elements	Conc before treatment (mg/L)	Conc after treatment (mg/L)	% of heavy metal removal
Fe	19.04	0.69	96.4
Mn	0.60	0.25	58.3
Zn	10.80	8.30	23.1

Fig. 6. (a) Histogram showing the removal percentage of Fe, Mn, and Zn from aquaculture wastewater effluent after treatment with biogenic FeNPs. (b) Concentration table of Fe, Mn, and Zn in aquaculture wastewater effluent before and after biogenic FeNPs treatment.

3.5. Cell viability of HepG2 and MDA-MB-231 cell lines treated with biogenic FeNPs

Treatment with biogenic FeNPs resulted in a dose-dependent decrease in cell viability for both HepG2 and MDA-MB-231 cell lines. In HepG2 cells (Figure 7a), cell viability remained high at lower concentrations (0.5–2 µg/mL), with only a slight reduction from 99.3% to 97.2 %. However, as the concentration increased from 4 to 16 µg/mL, a noticeable decline in viability was observed, reaching approximately 91.6% at the highest concentration. The calculated IC_{50} value for HepG2 cells was 6.338 mM, indicating low cytotoxicity within the tested concentration range.

A more pronounced cytotoxic effect was observed in MDA-MB-231 cells (Figure 7b). While cell viability remained above 90% at 0.5 and 1 µg/mL, a sharper reduction was evident at higher concentrations. At 8 µg/mL, viability dropped to around 89.1%; at 16 µg/mL, it further

ARTICLE IN PRESS

decreased to approximately 87.5%. The IC_{50} values were 2.538 mM, confirming a similarly low level of cytotoxicity.

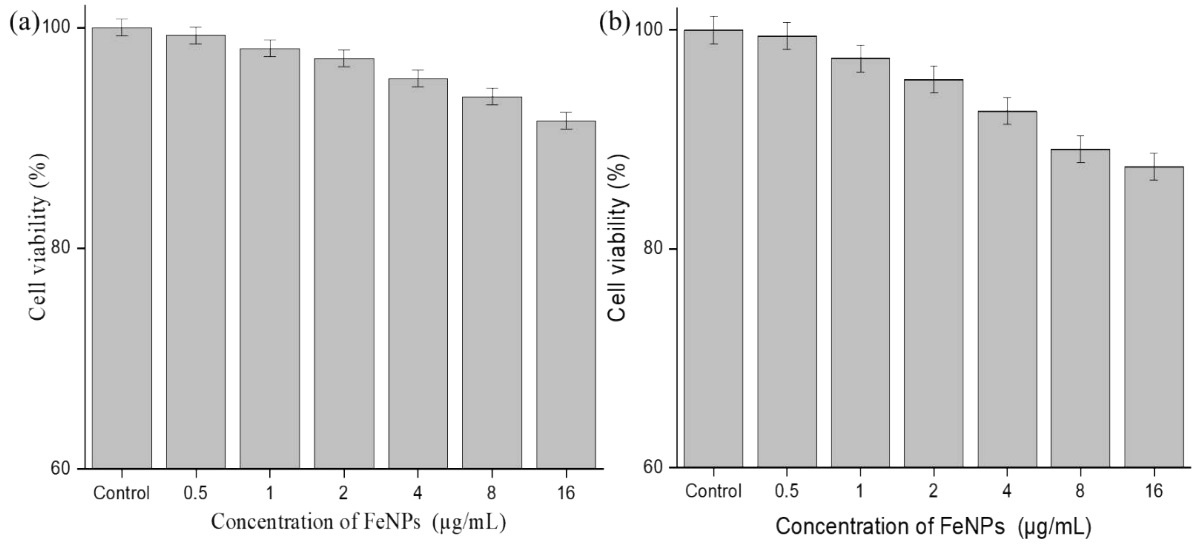


Fig. 7. Cell viability of (a) Human liver (HepG2) cells and (b) Human Breast Cancer (MDA-MB-231) cell lines treated with different concentrations of biogenic FeNPs (from 0.5 to 16 µg/ml). Error bars represent standard deviation [14].

Figures 8 and 9 illustrate the dose-dependent cytotoxic effects of biogenic FeNPs on HepG2 and MDA-MB-231 cell lines, respectively. In both cell types, the untreated controls (Figures 8a and 9a) displayed healthy morphology with well-spread, adherent cells and intact monolayers. After treatment with 4 µg/mL of FeNPs (Figures 8b and 9b), early morphological alterations such as slight rounding and reduced cell density appeared. These changes became more pronounced at 8 µg/mL (Figures 8c and 9c), where a clear increase in cell detachment and shrinkage was observed, indicating loss of membrane integrity and initiation of cell death pathways. At the highest concentration (16 µg/mL), both HepG2 and MDA-MB-231 cells (Figures 8d and 9d) showed significant morphological damage, including cell rounding, fragmentation, and sparse adherence, suggesting advanced cytotoxic effects likely due to apoptosis or necrosis.

ARTICLE IN PRESS

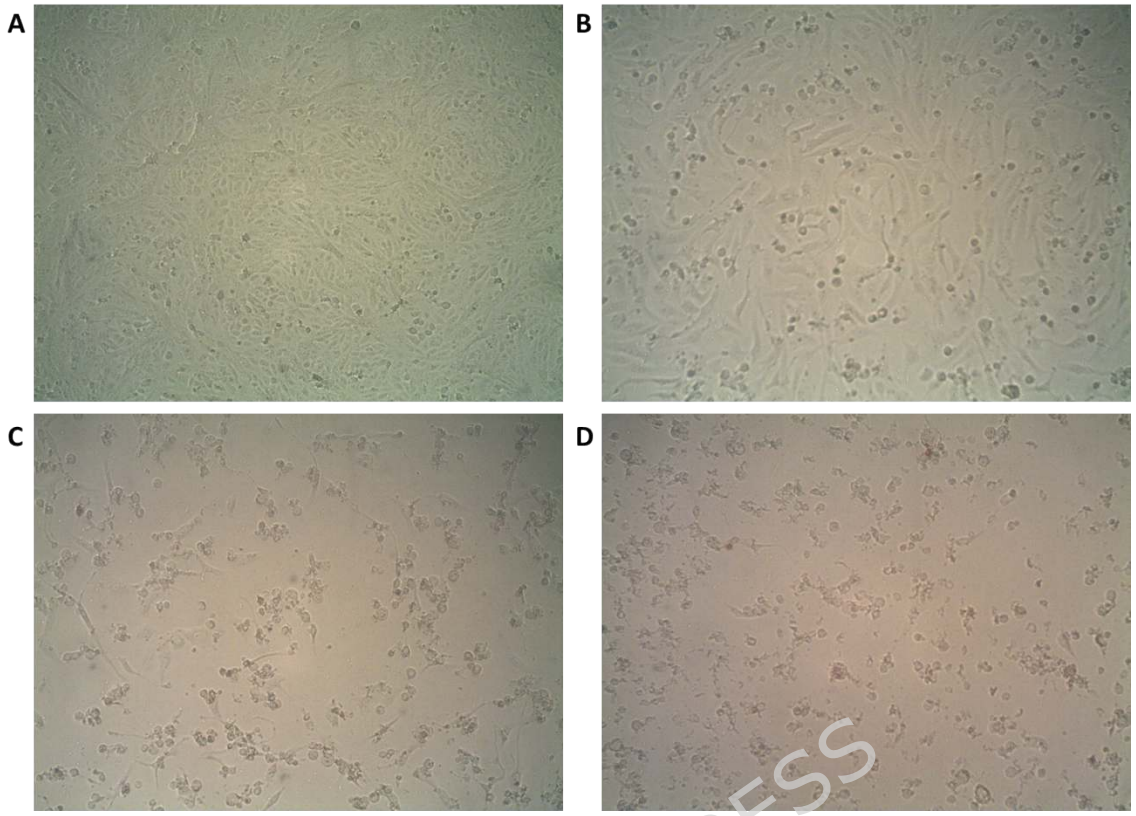


Fig. 8. Morphological changes of Human liver (HepG2) cells after treatment with biogenic FeNPs at different concentrations: (a) Control (untreated), (b) 4 µg/mL, (c) 8 µg/mL, and (d) 16 µg/mL.

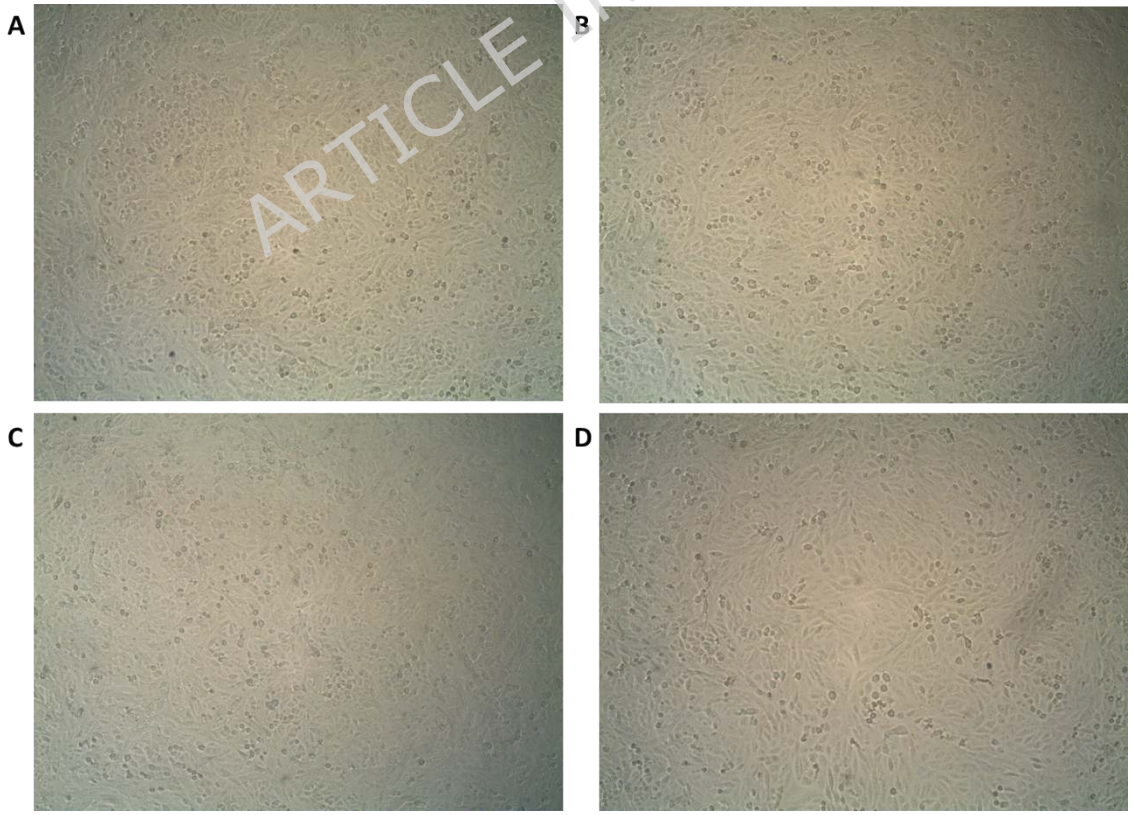


Fig. 9. Morphological changes of Human Breast Cancer (MDA-MB-231) cell lines after treatment with biogenic FeNPs at different concentrations: (a) Control (untreated), (b) 4 µg/mL, (c) 8 µg/mL, and (d) 16 µg/mL.

ARTICLE IN PRESS

4. Discussion

The present study demonstrates the successful biogenic synthesis of FeNPs using the red macroalga *Laurencia papillosa*, highlighting their dual environmental and biomedical applications. This green synthesis approach is environmentally friendly and cost-effective, as it relies on natural, non-toxic biomolecules, reduces chemical waste, and requires minimal energy input, supporting sustainable and scalable nanoparticle production [15]. The XRD pattern of the biogenic FeNPs revealed an amorphous nature, which aligns with several earlier reports on biogenically synthesized nanoparticles using algal or plant extracts [33,34]. The absence of sharp diffraction peaks is likely attributed to the strong organic capping provided by the bioactive compounds present in the *L. papillosa* extract. These biomolecules, such as polysaccharides, phenolics, and halogenated metabolites, can bind to the nanoparticle surface, hindering the formation of long-range crystalline order and thereby resulting in an amorphous structure [16]. The broad peak shown around 2θ of 20°−30° could correspond to the coated organic materials from *L. papillosa,* which are responsible for stabilizing the phyco-synthesized FeNPs [36]. Amorphous nanoparticles often exhibit higher surface reactivity, which could enhance their interaction with heavy metals or biological systems, making them highly suitable for applications such as water purification and targeted drug delivery [35]. This increased reactivity arises from the presence of structural disorder, surface defects, and unsaturated coordination sites, which provide a greater number of active binding sites. Consequently, amorphous FeNPs may show enhanced adsorption efficiency and stronger interactions with cellular membranes, potentially contributing to improved cytotoxic or biological activity [17]. The color change from yellowish-brown to deep brown upon the addition of $FeCl_3$ offers a visual indication of nanoparticle formation, as a result of the reduction of Fe^{3+} ions by bioactive compounds present in the algal extract. This observation is consistent with the general principle of green nanoparticle synthesis, where phytochemicals such as phenolics,

ARTICLE IN PRESS

flavonoids, terpenoids, and polysaccharides act as both reducing and stabilizing agents [37].

FTIR analysis further confirmed the involvement of functional groups in the synthesis and stabilization of FeNPs [38]. The prominent peak at 3421 cm^{-1} corresponds to O-H and N-H stretching vibrations, indicating the presence of hydroxyl and amine groups, which are known to play a key role in metal ion reduction and nanoparticle stabilization [39]. The peaks at 1598 and 1384 cm^{-1} are likely associated with C=O stretching and symmetric COO^- vibrations, respectively, suggesting the involvement of carboxyl-containing biomolecules in capping the nanoparticles [40]. The band at 1035 cm^{-1} may correspond to C-O stretching, while the peak at 865 cm^{-1} could be attributed to Fe-O vibrations, confirming the presence of iron in the synthesized nanoparticles [41]. Although the FTIR spectra of *L. papillosa* extract and FeNPs showed similar overall patterns, the observed differences in peak intensity indicate the participation of these functional groups in the reduction and stabilization processes. Similar spectral shifts and intensity changes have been reported by other researchers using marine algae and plant-based systems for nanoparticle synthesis, further validating the active role of biomolecules in nanoparticle formation [42,43].

The TEM analysis confirmed that the FeNPs were nearly spherical and polydispersed, with particle sizes ranging between 10.17 and 19.99 nm. This size range is consistent with earlier reports of biogenic FeNPs synthesized using algal or plant extracts [44,45]. Compared to previous similar studies, the nanoparticles in this study were smaller in size than other iron NPs, which have a size between 50–100 nm [18]. This variation may be attributed to differences in pH, temperature, incubation duration, as well as the nature and concentration of the precursors, all of which can significantly affect nanoparticle biosynthesis [19]. The SAED pattern, showing distinct concentric rings and discrete spots, confirmed the polycrystalline nature of the synthesized FeNPs. Such patterns have also

ARTICLE IN PRESS

been reported in other studies involving biologically mediated synthesis of metal nanoparticles [46].

The EDAX analysis further supported the elemental composition of the FeNPs, where prominent peaks corresponding to Fe were detected at 0.5, 6.0, and 6.6 keV. This finding is in agreement with previously published EDAX spectra of biosynthesized FeNPs [23]. The minor peaks corresponding to C, O, Na, Mg, Al, Cl, K, Cu, and Zn likely originate from residual biomolecules and trace salts present in the *Laurencia papillosa* extract, which act as natural capping and stabilizing agents for the FeNPs [20]. Their presence contributes to nanoparticle stability and surface reactivity but does not interfere with the overall composition or functionality of the FeNPs [21]. The absence of strong peaks for other elements also supports the high purity of the synthesized particles.SEM imaging revealed a spherical and highly polydispersed morphology, aligning with the TEM observations. Similar FeNPs were also reported [47].

The positive zeta potential value of +7.4 mV indicates moderate colloidal stability, which is attributed to the capping effect of negatively charged functional groups from the *Laurencia papillosa* extract. While higher absolute zeta potential values typically suggest better stability, previous studies have shown that even moderately positive zeta potentials can be sufficient to prevent significant aggregation, especially when natural stabilizers are present [48]. Earlier reports on nanoparticles synthesized via *L. papillosa* indicate stability patterns that align with those observed in this study [22]. This moderate positive charge also suggests that the FeNPs may exhibit favorable interactions with negatively charged contaminants or biomolecules, enhancing their adsorption capacity and biological activity [23].

The optimization study revealed that pH and algal concentration were the most significant factors affecting FeNPs synthesis, while incubation time had a minimal effect. These findings are consistent with previous studies [49]. The effect of pH and algal concentration directly

ARTICLE IN PRESS

controls the reduction kinetics of Fe^{3+} ions and the availability of active biomolecules responsible for reduction and capping [24]. Variations in pH alter the ionization state of phenolic, polysaccharide, and protein functional groups, thereby affecting their reducing capacity and binding efficiency [25]. Similarly, increasing algal extract concentration increases the number of bioactive compounds available to reduce and stabilize iron nanoparticles, leading to more efficient nanoparticle formation [26]. In contrast, incubation time exhibited a minimal effect, likely because the reduction of Fe^{3+} and nucleation of FeNPs occur rapidly once optimal biochemical conditions are present. Most of the nanoparticle formation appears to occur in the early stages of the reaction, and extending the time does not significantly alter the particle yield or properties [26].

Furthermore, the model's accuracy, validated by ANOVA and normal distribution of residuals, aligns with statistical approaches used in recent biosynthesis studies for predictive optimization [50]. The P value was found to be significant, and the assumption of standard data was almost normal. The proposed linear model is acceptable as it is lower than the permitted range of $\pm 3\sigma$ [51].

The high removal efficiency of Fe (96.4%) observed in this study highlights the strong potential of biogenic FeNPs, consistent with earlier studies that reported efficient heavy metal adsorption using green-synthesized nanoparticles [52,53]. The moderate removal of Mn (58.3%) and Zn (23.1%) also aligns with previous findings indicating variable affinity of FeNPs toward different metal ions depending on their ionic radii, charge, and binding behavior [54]. The high removal efficiency of FeNPs is attributed to their small size and large surface area, enabling effective surface adsorption, electrostatic attraction, and complexation with functional groups from the *Laurencia papillosa* extract [27]. The moderate positive surface charge enhances interaction with metal ions, improves removal efficiency [23]. The observed trend-greater affinity for Fe than Mn and Zn, may be attributed to the redox reactivity of FeNPs and their strong binding with iron species in solution. Similar outcomes have been reported

ARTICLE IN PRESS

in studies using algae-based or plant-extract-mediated FeNPs, where the surface functional groups contribute to metal chelation and reduction [55].

Numerous studies have demonstrated that the bioactive compounds derived from algae and marine plants exhibit anticancer activity against various cancer cell lines [56,57]. The observed dose-dependent morphological alterations in HepG2 and MDA-MB-231 cells following exposure to biogenic FeNPs are consistent with earlier findings that highlight the cytotoxic potential of iron-based nanoparticles against cancer cells [58,59]. Studies using green-synthesized FeNPs, such as those derived from algae or plant extracts, have similarly demonstrated selective cytotoxic effects on cancerous cells while sparing normal cells to a greater extent [60,61]. The observed dose-dependent cytotoxicity of the synthesized FeNPs against HepG2 and MDA-MB-231 cells may be attributed to their small size, positive surface charge, and bioactive compounds from *Laurencia papillosa*. These properties facilitate cellular uptake and can induce reactive oxygen species (ROS) generation, leading to oxidative stress, mitochondrial dysfunction, and apoptosis in cancer cells [28]. The results suggest that biogenic FeNPs exhibit selective cytotoxicity, with a stronger inhibitory effect on MDA-MB-231 compared to HepG2, especially at higher concentrations. The stronger response of MDA-MB-231 cells may reflect the higher metabolic activity and sensitivity of breast cancer cells to oxidative stress, as previously noted by Nasrollahzadeh, *et al.* [29]. In comparison with standard anticancer drugs, the biogenic FeNPs evaluated in this study demonstrated markedly lower cytotoxicity toward both HepG2 and MDA-MB-231 cells [30]. The high IC_{50} of the biogenic FeNPs compared to conventional chemotherapeutic agents such as doxorubicin and cisplatin reflects their lower cytotoxic potency but also their greater safety [31]. Similar low-to-moderate cytotoxicity has been reported for other biosynthesized iron nanoparticles, likely due to organic capping by algal biomolecules, aligning our findings with previous studies and supporting the safe biomedical potential of these FeNPs [32,33]. Additionally, the presence of bioactive capping agents from *Laurencia papillosa* likely enhanced cellular uptake and internal disruption, supporting the dual

ARTICLE IN PRESS

therapeutic and environmental applications of such biogenic nanoparticles. Overall, these findings demonstrate that the eco-friendly synthesis and applications of the FeNPs contribute to several SDGs. Specifically, SDG 6 (Clean Water and Sanitation) is addressed through potential water remediation applications, SDG 3 (Good Health and Well-Being) is supported via prospective biomedical and targeted cancer treatments, and SDG 12 (Responsible Consumption and Production) is promoted by employing sustainable and green nanotechnology practices. Finally, Table 4 summarizes and compares the present study with previously reported biogenic FeNPs synthesized using different biological sources. The comparison highlights variations in synthesis approaches, particle size ranges, morphological features, and application domains. As shown, most earlier studies focused on single-purpose applications, either environmental or biomedical, whereas the present work demonstrates dual functionality using a marine algal source. This comparison underscores the relevance of *Laurencia papillosa*-mediated FeNPs and supports their potential as multifunctional nanomaterials.

Table 4. Comparative overview of biogenic iron nanoparticles (FeNPs) synthesized using different biological sources, showing synthesis method, particle size, shape, applications, and references.

Biological Source	Synthesis Method	Particle Size (nm)	Shape	Application(s)	Reference
Laurencia papillosa (red marine alga)	Biogenic, RSM-optimized	10.17-19.99	Spherical	Heavy metal removal, anticancer activity	**Present Study**
Azadirachta indica (leaf extract)	Biogenic	12-25	Spherical / Polydispersed	Anti-bacterial activity	[34]
Ficus carica (fruit extract)	Biogenic	15-30	Spherical	Anticancer	[35]
Bacillus subtilis (bacteria)	Biogenic	8-20	Spherical	Heavy metal removal	[36]
Pleurotus citrinopileatus (fungus)	Biogenic	20-40	Spherical / Irregular	Biomedical application	[37]

5. Limitations and Strengths of the Study

ARTICLE IN PRESS

This study demonstrates an eco-friendly and cost-effective synthesis of FeNPs using *Laurencia papillosa*, with comprehensive characterization confirming their structural, morphological, and functional properties. The dual applications in environmental remediation and biomedical contexts represent a major strength, highlighting the multifunctional potential of these biogenic nanoparticles. However, the study has some limitations, including: reliance on in vitro assessments without in vivo validation, limited mechanistic insights into cytotoxicity and heavy metal adsorption, and absence of scale-up studies and long-term stability evaluations under diverse environmental conditions. Future studies addressing these aspects would further validate the practical applications of the synthesized FeNPs and expand their utility in both environmental and biomedical fields.

6. Conclusions

This study successfully demonstrated the biogenic synthesis of iron nanoparticles (FeNPs) using the red marine alga *Laurencia papillosa*, providing a sustainable and eco-friendly approach to nanoparticle production. The synthesized FeNPs were small, spherical, and polycrystalline with favorable surface properties, and optimization showed that pH and algal concentration significantly influenced nanoparticle formation. The FeNPs exhibited high efficiency in removing heavy metals (Fe, Mn, and Zn) from aquaculture wastewater, highlighting their environmental application. Additionally, they showed dose-dependent cytotoxicity against HepG2 and MDA-MB-231 cancer cell lines, suggesting potential utility in cancer therapy. The study is limited by the number of replicates, the lack of detailed adsorption modeling, and the absence of in vivo validation. Future work will focus on mechanistic studies, adsorption modeling, in vivo biodistribution, toxicity, and biocompatibility to further establish the multifunctional potential of these eco-friendly FeNPs in both environmental remediation and biomedical applications.

ARTICLE IN PRESS

Data availability

The data will be provided by the corresponding author upon reasonable request.

ARTICLE IN PRESS

Conflict of interest

The authors declare no conflict of interest.

Funding

The financial support for this research was provided by the Science, Technology & Innovation Funding Authority (STDF), Egypt through a Post Graduate Support Grant (PGSG), Non-Industrial sector, National, grant number 45049.

CRediT authorship contribution statement

Ahlam S. El Shehawy conducted the experiments and drafted the manuscript with guidance and support from the co-authors. Elham M. Ali and Ashraf Elsayed verified the analytical methods and validated the numerical results. They were also involved in planning the study and supervising the overall work. All authors contributed to the discussion of the results and provided feedback on the manuscript.

References

1. Abel, S. *et al.* Application of titanium dioxide nanoparticles synthesized by sol-gel methods in wastewater treatment. *Journal of Nanomaterials* **2021**, 1-6 (2021).
2. Joseph, T. M., Al-Hazmi, H. E., Śniatała, B., Esmaeili, A. & Habibzadeh, S. Nanoparticles and nanofiltration for wastewater treatment: From polluted to fresh water. *Environmental Research*, 117114 (2023).
3. Viswanathan, S. *et al.* Synthesis, characterization, cytotoxicity, and antimicrobial studies of green synthesized silver nanoparticles using red seaweed *Champia parvula*. *Biomass Conversion and Biorefinery*, 1-14 (2023).
4. Ameen, F., Al-Maary, K. S., Almansob, A. & AlNadhari, S. Antioxidant, antibacterial and anticancer efficacy of *Alternaria chlamydospora*-mediated gold nanoparticles. *Applied Nanoscience* **13**, 2233-2240 (2023).
5. Fahmy, H. M. *et al.* Review of green methods of iron nanoparticles synthesis and applications. *Bionanoscience* **8**, 491-503 (2018).
6. Mostafazade, R., Arabi, L., Tazik, Z., Akaberi, M. & Bazzaz, B. S. F. Green synthesis of gold, copper, zinc, iron, and other metal nanoparticles by fungal endophytes; characterization, and their biological activity: a review. *Biocatalysis and Agricultural Biotechnology*, 103307 (2024).
7. Jeyaraj, M., Gurunathan, S., Qasim, M., Kang, M.-H. & Kim, J.-H. A Comprehensive Review on the Synthesis, Characterization, and Biomedical Application of Platinum Nanoparticles. *Nanomaterials* **9**, 1719 (2019).
8. Naseem, K. *et al.* Biogenic synthesized nanocatalysts and their potential for the treatment of toxic pollutants: environmental remediation, a review. *International Journal of Environmental Science and Technology* **21**, 2163-2194 (2024).
9. Singaravelu, G., Arockiamary, J., Kumar, V. G. & Govindaraju, K. A novel extracellular synthesis of monodisperse gold nanoparticles using marine alga,

ARTICLE IN PRESS

Sargassum wightii Greville. *Colloids and surfaces B: Biointerfaces* **57**, 97-101 (2007).
10. Wen, J. *et al.* Metallic nanoparticles synthesized by algae: Synthetic route, action mechanism, and the environmental catalytic applications. *Journal of Environmental Chemical Engineering* **12**, 111742 (2024).
11. Chan, S. S. *et al.* Prospects and environmental sustainability of phyconanotechnology: A review on algae-mediated metal nanoparticles synthesis and mechanism. *Environmental research* **212**, 113140 (2022).
12. El Shehawy, A. S., Elsayed, A., El-Shehaby, O. A. & Ali, E. M. Potentiality of the green synthesized silver nanoparticles for heavy metal removal using *Laurencia* papillosa seaweed. *The Egyptian Journal of Aquatic Research*, doi:doi.org/10.1016/j.ejar.2023.10.001 (2023).
13. Water, U. Water for a sustainable world. *The United Nations World Water Development Report* (2015).
14. Owa, F. Water pollution: sources, effects, control and management. *International Letters of Natural Sciences* **3** (2014).
15. Emmanuel, U. C., Chukwudi, M. I., Monday, S. S. & Anthony, A. I. Human health risk assessment of heavy metals in drinking water sources in three senatorial districts of Anambra State, Nigeria. *Toxicology Reports* **9**, 869-875 (2022).
16. Society, A. Global cancer facts and figures 4th edition. *Am Cancer Soc* **1**, 1-73 (2018).
17. Andleeb, A. *et al.* A systematic review of biosynthesized metallic nanoparticles as a promising anti-cancer-strategy. *Cancers* **13**, 2818 (2021).
18. Al-Khedhairy, A. A. & Wahab, R. Silver nanoparticles: An instantaneous solution for anticancer activity against human liver (HepG2) and breast (MCF-7) cancer cells. *Metals* **12**, 148 (2022).
19. Sangour, M. H., Ali, I. M., Atwan, Z. W. & Al Ali, A. A. A. L. A. Effect of Ag nanoparticles on viability of MCF-7 and Vero cell lines and gene expression of apoptotic genes. *Egyptian Journal of Medical Human Genetics* **22**, 1-11 (2021).
20. El-Sheekh, M. M., Hassan, L. H. & Morsi, H. H. Assessment of the in vitro anticancer activities of cyanobacteria mediated silver oxide and gold nanoparticles in human colon CaCo-2 and cervical HeLa cells. *Environmental Nanotechnology, Monitoring & Management* **16**, 100556 (2021).
21. Zhang, Y. *et al.* Green formulation, chemical characterization, and antioxidant, cytotoxicity, and anti-human cervical cancer effects of vanadium nanoparticles: A pre-clinical study. *Arabian Journal of Chemistry* **14**, 103147 (2021).
22. Lima, A., Gaspar, R., Neto, J. & Pereira, L. The identification of macroalgae and the assessment of intertidal rocky shores' ecological statuses in the central western coast of continental Portugal, Chapter 2. *Seaweeds Biodiversity, environmental chemistry and ecological impacts. Hauppauge, New-York: Nova Science Publishers, Inc*, 19-84 (2017).
23. Mahdavi, M., Namvar, F., Ahmad, M. B. & Mohamad, R. Green biosynthesis and characterization of magnetic iron oxide (Fe3O4) nanoparticles using seaweed (*Sargassum muticum*) aqueous extract. *Molecules* **18**, 5954-5964 (2013).
24. Al-Zahrani, S. A. *et al.* Green-synthesized silver nanoparticles with aqueous extract of green algae *Chaetomorpha ligustica* and its anticancer potential. *Green Processing and Synthesis* **10**, 711-721 (2021).
25. Bachheti, R. K., Abate, L., Bachheti, A., Madhusudhan, A. & Husen, A. in *Handbook of greener synthesis of nanomaterials and compounds* 701-734 (Elsevier, 2021).
26. Soureshjani, P. T., Shadi, A. & Mohammadsaleh, F. Algae-mediated route to biogenic cuprous oxide nanoparticles and spindle-like CaCO 3: a comparative

ARTICLE IN PRESS

study, facile synthesis, and biological properties. *RSC advances* **11**, 10599-10609 (2021).
27. Alprol, A. E., Mansour, A. T., El-Beltagi, H. S. & Ashour, M. Algal extracts for green synthesis of zinc oxide nanoparticles: promising approach for algae bioremediation. *Materials* **16**, 2819 (2023).
28. Brindhadevi, K. *et al.* Central composite design for the optimization of CaO and Fe2 (SO4) 3 facilitated transesterification of Scenedesmus sp. oil for fatty acid methyl ester production. *Fuel* **321**, 124096 (2022).
29. Karimi, P., Javanshir, S., Sayadi, M. H. & Arabyarmohammadi, H. Arsenic removal from mining effluents using plant-mediated, green-synthesized iron nanoparticles. *Processes* **7**, 759 (2019).
30. Ahamed, M. *et al.* Oxidative stress mediated apoptosis induced by nickel ferrite nanoparticles in cultured A549 cells. *Toxicology* **283**, 101-108 (2011).
31. Mohamed, R. M. *et al.* Production, characterization, and cytotoxicity effects of silver nanoparticles from Brown alga (*Cystoseira myrica*). *Journal of Nanotechnology* **2022**, 6469090 (2022).
32. Macías Sánchez, K. L., González Martínez, H. D. R., Carrera Cerritos, R. & Martínez Espinosa, J. C. In Vitro Evaluation of the Antifungal Effect of AgNPs on *Fusarium oxysporum f. sp. lycopersici*. *Nanomaterials* **13**, 1274 (2023).
33. Kouhbanani, M. A. J., Beheshtkhoo, N., Taghizadeh, S., Amani, A. M. & Alimardani, V. One-step green synthesis and characterization of iron oxide nanoparticles using aqueous leaf extract of *Teucrium polium* and their catalytic application in dye degradation. *Advances in Natural Sciences: Nanoscience and Nanotechnology* **10**, 015007 (2019).
34. Makarov, V. V. *et al.* Biosynthesis of stable iron oxide nanoparticles in aqueous extracts of *Hordeum vulgare* and *Rumex acetosa* plants. *Langmuir* **30**, 5982-5988 (2014).
35. Li, S. *et al.* Mn MOF-derivatives synthesized based upon a mechanochemistry method for low-temperature NH3-SCR: From amorphous precursor to amorphous catalyst. *Molecular Catalysis* **554**, 113767 (2024).
36. Barcelos, K. A., Tebaldi, M. L., do Egito, E. S. T., Leão, N. M. & Soares, D. C. F. PEG-Iron Oxide Core-Shell Nanoparticles: In situ Synthesis and In vitro Biocompatibility Evaluation for Potential T 2-MRI Applications. *Bionanoscience* **10**, 1107-1120 (2020).
37. Alamu, G. A. *et al.* Green synthesis and characterizations of magnetic iron oxide nanoparticles using *Moringa oleifera* extract for improved performance in dye-sensitized solar cell. *Chemical Physics Impact* **8**, 100542 (2024).
38. Malik, M. A., Alshehri, A. A. & Patel, R. Facile one-pot green synthesis of Ag–Fe bimetallic nanoparticles and their catalytic capability for 4-nitrophenol reduction. *Journal of Materials Research and Technology* **12**, 455-470 (2021).
39. Balaraman, P. *et al.* Phyco-synthesis of silver nanoparticles mediated from marine algae *Sargassum myriocystum* and its potential biological and environmental applications. *Waste and Biomass Valorization* **11**, 5255-5271 (2020).
40. Venkateswarlu, S., Kumar, B. N., Prathima, B., SubbaRao, Y. & Jyothi, N. V. V. A novel green synthesis of Fe3O4 magnetic nanorods using *Punica Granatum rind* extract and its application for removal of Pb [38] from aqueous environment. *Arabian Journal of Chemistry* **12**, 588-596 (2019).
41. Shanmugam, R., Tharani, M., Abullais, S. S., Patil, S. R. & Karobari, M. I. Black seed assisted synthesis, characterization, free radical scavenging, antimicrobial and anti-inflammatory activity of iron oxide nanoparticles. *BMC Complementary Medicine and Therapies* **24**, 241 (2024).
42. Salem, D. M., Ismail, M. M. & Aly-Eldeen, M. A. Biogenic synthesis and antimicrobial potency of iron oxide (Fe3O4) nanoparticles using algae harvested

ARTICLE IN PRESS

from the Mediterranean Sea, Egypt. *The Egyptian Journal of Aquatic Research* **45**, 197-204 (2019).
43. Algotiml, R. *et al.* Anticancer and antimicrobial activity of biosynthesized Red Sea marine algal silver nanoparticles. *Scientific reports* **12**, 1-18 (2022).
44. Sathishkumar, G. *et al.* Green synthesis of magnetic Fe3O4 nanoparticles using *Couroupita guianensis Aubl*. fruit extract for their antibacterial and cytotoxicity activities. *Artificial cells, nanomedicine, and biotechnology* **46**, 589-598 (2018).
45. Elsayed, A., Ali, E. & El Shehawy, A. Algae-Mediated Synthesis and Structural Characterization of Iron Nanoparticles using *Galaxaura rugosa* Seaweed. *Egyptian Journal of Phycology* (2024).
46. Sathiyaraj, S. *et al.* Biosynthesis, characterization, and antibacterial activity of gold nanoparticles. *Journal of Infection and Public Health* **14**, 1842-1847 (2021).
47. Mathur, P., Saini, S., Paul, E., Sharma, C. & Mehtani, P. Endophytic fungi mediated synthesis of iron nanoparticles: Characterization and application in methylene blue decolorization. *Current Research in Green and Sustainable Chemistry* **4**, 100053 (2021).
48. Bhattacharjee, S. DLS and zeta potential–what they are and what they are not? *Journal of controlled release* **235**, 337-351 (2016).
49. Laid, T. M., Abdelhamid, K., Eddine, L. S. & Abderrhmane, B. Optimizing the biosynthesis parameters of iron oxide nanoparticles using central composite design. *Journal of Molecular Structure* **1229**, 129497 (2021).
50. Chowdhury, S., Yusof, F., Faruck, M. O. & Sulaiman, N. Process optimization of silver nanoparticle synthesis using response surface methodology. *Procedia engineering* **148**, 992-999 (2016).
51. Ibrahim, S. *et al.* Optimization for biogenic microbial synthesis of silver nanoparticles through response surface methodology, characterization, their antimicrobial, antioxidant, and catalytic potential. *Scientific Reports* **11**, 770 (2021).
52. Devatha, C., Thalla, A. K. & Katte, S. Y. Green synthesis of iron nanoparticles using different leaf extracts for treatment of domestic waste water. *Journal of cleaner production* **139**, 1425-1435 (2016).
53. Fahmy, H. M. *et al.* Review of green methods of iron nanoparticles synthesis and applications. *BioNanoScience* **8**, 491-503 (2018).
54. Suresh, A. K., Pelletier, D. A. & Doktycz, M. J. Relating nanomaterial properties and microbial toxicity. *Nanoscale* **5**, 463-474 (2013).
55. Al-Saad, K. *et al.* Iron oxide nanoparticles: applicability for heavy metal removal from contaminated water. *Arab Journal of Nuclear Sciences and Applications* **45**, 335-346 (2012).
56. Baskar, G. *et al.* Biosynthesis of iron oxide nanoparticles from red seaweed *Hypnea valentiae* and evaluation of their antioxidant and antitumor potential via the AKT/PI3K pathway. *Process Biochemistry* **141**, 155-169 (2024).
57. Hajri, A. K., Albalawi, M. A., Alsharif, I. & Jamoussi, B. Marine algae extract (*Grateloupia Sparsa*) for the green synthesis of Co3O4NPs: antioxidant, antibacterial, anticancer, and hemolytic activities. *Bioinorganic Chemistry and Applications* **2022**, 3977935 (2022).
58. Palaniyandi, T. *et al.* Biosynthesis of iron nanoparticles using brown algae *Spatoglossum asperum* and its antioxidant and anticancer activities through in vitro and in silico studies. *Particulate Science and Technology* **41**, 916-929 (2023).
59. Jafari, N., Hamishehkar, H. & Mohammadpourfard, M. *Dunaliella* salina microalgae aqueous extract-based magnetic nanoparticles (Fe3O4-NPs): Green

ARTICLE IN PRESS

synthesis, characterization and in vitro anticancer investigations. *Algal Research* **80**, 103560 (2024).
60. Ali, M., Anuradha, V., Abishek, R., Yogananth, N. & Sheeba, H. In vitro anticancer activity of green synthesis ruthenium nanoparticle from *Dictyota dichotoma* marine algae. *NanoWorld J* **3**, 66-71 (2017).
61. Salam, A. S. A., Anchan, R. V., Murugan, S. S., Majhi, D. & Venkatesan, J. in *Nano-formulation of Dietary Phytochemicals for Cancer Management* 327-347 (Springer, 2025).
62. Nasrollahzadeh, A. *et al.* Arsenic trioxide and BIBR1532 synergistically inhibit breast cancer cell proliferation through attenuation of NF-κB signaling pathway. *Life sciences* **257**, 118060 (2020).

1. Sharma, A. *et al.* Algae as crucial organisms in advancing nanotechnology: a systematic review. *Journal of applied phycology* **28**, 1759-1774 (2016).
2. Fahmy, H. M. *et al.* Review of green methods of iron nanoparticles synthesis and applications. *Bionanoscience* **8**, 491-503 (2018).
3. El Shehawy, A. S., Elsayed, A., El-Shehaby, O. A. & Ali, E. M. Potentiality of the green synthesized silver nanoparticles for heavy metal removal using Laurencia papillosa seaweed. *The Egyptian Journal of Aquatic Research*, doi:doi.org/10.1016/j.ejar.2023.10.001 (2023).
4. Mahmood Ansari, S. *et al.* Marine macroalgae display bioreductant efficacy for fabricating metallic nanoparticles: intra/extracellular mechanism and potential biomedical applications. *Bioinorganic Chemistry and Applications* **2021**, 5985377 (2021).
5. Premarathna, K. *et al.* Greening up the fight against emerging contaminants: algae-based nanoparticles for water remediation. *Clean Technologies and Environmental Policy* **27**, 5825-5842 (2025).
6. Omar, H. H., Bahabri, F. S. & El-Gendy, A. M. Biopotential application of synthesis nanoparticles as antimicrobial agents by using Laurencia papillosa. *International Journal of Pharmacology* **13**, 303-312 (2017).
7. Bensy, A. D., Christobel, G. J., Muthusamy, K., Alfarhan, A. & Anantharaman, P. Green synthesis of iron nanoparticles from Ulva lactuca and bactericidal activity against enteropathogens. *Journal of King Saud University-Science* **34**, 101888 (2022).
8. Mahdavi, M., Namvar, F., Ahmad, M. B. & Mohamad, R. Green biosynthesis and characterization of magnetic iron oxide (Fe3O4) nanoparticles using seaweed (Sargassum muticum) aqueous extract. *Molecules* **18**, 5954-5964 (2013).
9. Ganesan, M. *et al.* Biosynthesis and characterization of Lissachatina fulica snail mucus (LfSM)-mediated iron oxide (Fe2O3) nanoparticles: antibacterial and anticancer efficiency. *South African Journal of Botany* **175**, 732-743 (2024).
10. Kumar, P., Govindaraju, M., Senthamilselvi, S. & Premkumar, K. Photocatalytic degradation of methyl orange dye using silver (Ag) nanoparticles synthesized from Ulva lactuca. *Colloids and Surfaces B: biointerfaces* **103**, 658-661 (2013).
11. Sharma, R., Bisen, D., Shukla, U. & Sharma, B. X-ray diffraction: a powerful method of characterizing nanomaterials. *Recent Res Sci Technol* **4**, 77-79 (2012).
12. Zou, Y. *et al.* Environmental remediation and application of nanoscale zero-valent iron and its composites for the removal of heavy metal ions: a review. *Environmental science & technology* **50**, 7290-7304 (2016).
13. Pradhan, S. *Comparative analysis of Silver Nanoparticles prepared from Different Plant extracts (Hibiscus rosa sinensis, Moringa oleifera, Acorus calamus, Cucurbita maxima, Azadirachta indica) through green synthesis method*, (2013).
14. Macías Sánchez, K. L., González Martínez, H. D. R., Carrera Cerritos, R. & Martínez Espinosa, J. C. In Vitro Evaluation of the Antifungal Effect of AgNPs on Fusarium oxysporum f. sp. lycopersici. *Nanomaterials* **13**, 1274 (2023).

ARTICLE IN PRESS

15. Ali, E. M., Elsayed, A. & El Shehawy, A. S. A novel green biosynthesis approach and structural characterization of Ag–Fe bimetallic nanoparticles using the red alga Galaxaura rugosa. *Scientific Reports* **15**, 31129 (2025).
16. Barcelos, K. A., Tebaldi, M. L., do Egito, E. S. T., Leão, N. M. & Soares, D. C. F. PEG-Iron Oxide Core-Shell Nanoparticles: In situ Synthesis and In vitro Biocompatibility Evaluation for Potential T 2-MRI Applications. *Bionanoscience* **10**, 1107-1120 (2020).
17. Abdelghany, S., Elsayed, A., Kabary, H. & Salaheldin, H. Iron oxide/silver-doped iron oxide nanoparticles: facile synthesis, characterization, antibacterial activity, genotoxicity and anticancer evaluation. *Scientific Reports* **15**, 29593 (2025).
18. Xin, H. *et al.* Biosynthesis of iron nanoparticles using tie guanyin tea extract for degradation of bromothymol blue. *Journal of Nanotechnology* **2016** (2016).
19. Patra, J. K. & Baek, K.-H. Green nanobiotechnology: factors affecting synthesis and characterization techniques. *Journal of Nanomaterials* **2014** (2014).
20. Bhuyar, P. *et al.* Synthesis of silver nanoparticles using marine macroalgae Padina sp. and its antibacterial activity towards pathogenic bacteria. *Beni-Suef University Journal of Basic and Applied Sciences* **9**, 1-15 (2020).
21. Abdel-Raouf, N., Alharbi, R. M., Al-Enazi, N. M., Alkhulaifi, M. M. & Ibraheem, I. B. M. Rapid biosynthesis of silver nanoparticles using the marine red alga Laurencia catarinensis and their characterization. *Beni-Suef University Journal of Basic and Applied Sciences* **7**, 150-157 (2018).
22. Vemula, P. & Chatragadda, R. in *Ecofriendly and Multifunctional Nanoparticles* 1-135 (Springer, 2025).
23. El-Sheekh, M. M., El-Kassas, H. Y., Shams El-Din, N. G., Eissa, D. I. & El-Sherbiny, B. A. Green synthesis, characterization applications of iron oxide nanoparticles for antialgal and wastewater bioremediation using three brown algae. *International Journal of Phytoremediation* **23**, 1538-1552 (2021).
24. Ibrahim, S. *et al.* Optimization for biogenic microbial synthesis of silver nanoparticles through response surface methodology, characterization, their antimicrobial, antioxidant, and catalytic potential. *Scientific Reports* **11**, 770 (2021).
25. Mat Yusuf, S. N. A. *et al.* Optimization of biogenic synthesis of silver nanoparticles from flavonoid-rich Clinacanthus nutans leaf and stem aqueous extracts. *Royal Society open science* **7**, 200065 (2020).
26. Costa, L. *et al.* Green synthesis of gold nanoparticles obtained from algae Sargassum cymosum: optimization, characterization and stability. *BioNanoScience* **10**, 1049-1062 (2020).
27. Suresh, J. I. & Evangelina, A. in *Green Technologies for Wastewater Treatment and Bioenergy Production* 239-255 (CRC Press, 2025).
28. Karunanithi, B., Manimaran, K. & Srividhya, M. Isolation and characterization of amentoflavone-BSA coated polymer nanoparticles using Cassia fistula leaf extract against antibacterial and anticancer activity. *Biomass Conversion and Biorefinery* **14**, 16319-16328 (2024).
29. Nasrollahzadeh, A. *et al.* Arsenic trioxide and BIBR1532 synergistically inhibit breast cancer cell proliferation through attenuation of NF-κB signaling pathway. *Life sciences* **257**, 118060 (2020).
30. Olivier, T., Haslam, A. & Prasad, V. Anticancer drugs approved by the US Food and Drug Administration from 2009 to 2020 according to their mechanism of action. *JAMA network open* **4**, e2138793-e2138793 (2021).
31. Thurston, D. E. & Pysz, I. *Chemistry and pharmacology of anticancer drugs*. (CRC press, 2021).
32. Rukhsar, M. *et al.* An overview of iron oxide (Fe3O4) nanoparticles: from synthetic strategies, characterization to antibacterial and anticancer applications. *Crystals* **12**, 1809 (2022).
33. Palaniyandi, T. *et al.* Biosynthesis of iron nanoparticles using brown algae Spatoglossum asperum and its antioxidant and anticancer activities through in vitro and in silico studies. *Particulate Science and Technology* **41**, 916-929 (2023).

ARTICLE IN PRESS

34. Yilleng, T. *et al.* Biosynthesis of copper and iron nanoparticles using neem (Azadirachta indica) leaf extract and their anti-bacterial activity. *Journal of Applied Sciences and Environmental Management* **24**, 1987-1991 (2020).
35. Üstün, E., Önbaş, S. C., Çelik, S. K., Ayvaz, M. Ç. & Şahin, N. Green synthesis of iron oxide nanoparticles by using Ficus carica leaf extract and its antioxidant activity. *Biointerface Res. Appl. Chem* **12**, 2108-2116 (2022).
36. Khan, S., Akhtar, N., Rehman, S. U., Shujah, S. & Jamil, M. Iron oxide nanoparticle (Fe3O4 NPs) synthesized from B. subtilis reduced arsenic (as) toxicity in rice (Oryza sativa L.) plant. *International Journal of Phytoremediation* **26**, 1676-1682 (2024).
37. Manimaran, K. *et al.* Biological synthesis and characterization of iron oxide (FeO) nanoparticles using Pleurotus citrinopileatus extract and its biomedical applications. *Biomass Conversion and Biorefinery* **14**, 12575-12585 (2024).
38. Carroll, K. J. *et al.* One-pot aqueous synthesis of Fe and Ag core/shell nanoparticles. *Chemistry of Materials* **22**, 6291-6296 (2010).

ARTICLE IN PRESS